# Alternative splicing of the FGF antisense gene: Differential subcellular localization in human tissues and esophageal adenocarcinoma

**Article** *in* Journal of Molecular Medicine · December 2007

Impact Factor: 5.11 · DOI: 10.1007/s00109-007-0219-9 · Source: PubMed



**7 authors**, including:

Shuo Cheng Zhang
National Research Council Canada
**22** PUBLICATIONS **228** CITATIONS
SEE PROFILE

Laurette Geldenhuys
Dalhousie University
**27** PUBLICATIONS **502** CITATIONS
SEE PROFILE

Geoffrey Porter
Dalhousie University
**71** PUBLICATIONS **2,294** CITATIONS
SEE PROFILE

Paul R Murphy
Dalhousie University
**77** PUBLICATIONS **2,634** CITATIONS
SEE PROFILE

J Mol Med
DOI 10.1007/s00109-007-0219-9

ORIGINAL ARTICLE

# Alternative splicing of the FGF antisense gene: differential subcellular localization in human tissues and esophageal adenocarcinoma

**Shuo Cheng Zhang · Christie Barclay · Leigh Ann Alexander · Laurette Geldenhuys · Geoffrey A. Porter · Alan G. Casson · Paul R. Murphy**

Received: 20 January 2007 / Revised: 24 March 2007 / Accepted: 24 May 2007


**Abstract** Overexpression of FGF-2 is associated with tumor recurrence and reduced survival after surgical resection of esophageal cancer, and these risks are reduced in tumors co-expressing the FGF antisense (FGF-AS) RNA. The aim of this study was to characterize the expression of alternatively spliced FGF-AS transcripts and encoded nudix-motif proteins in normal human tissues and in esophageal adenocarcinoma, and to correlate their expression with clinicopathologic findings and outcome. Three alternatively spliced FGF-AS transcripts encoding GFG/NUDT6 isoforms with distinct N termini were detected in various human tissues including esophageal adenocarcinoma. Expression of each isoform as a fusion protein with enhanced green fluorescent protein revealed differential subcellular trafficking: hGFG*a* is localized to mitochondria by an N-terminal targeting sequence (MTS), whereas hGFG*b* and hGFG*c* were localized in the cytoplasm and nucleus. Mutation/deletion analysis confirmed that the predicted MTS was necessary and sufficient for mitochondrial compartmentalization. The predominant FGF-AS mRNA expressed in esophageal tumors was splice variant *b*. GFG immunoreactivity was detected in the cytoplasm of all esophageal adenocarcinomas and in 88% of tumor cell

S. C. Zhang · C. Barclay · L. A. Alexander · P. R. Murphy (✉)
Department of Physiology and Biophysics, Faculty of Medicine,
Dalhousie University,
5850 College Street,
Halifax, NS B3H 1X5, Canada
e-mail: prmurphy@dal.ca

L. Geldenhuys · A. G. Casson
Department of Pathology, Faculty of Medicine,
Dalhousie University,
5850 College Street,
Halifax, NS B3H 1X5, Canada

G. A. Porter · A. G. Casson
Department of Surgery, Faculty of Medicine,
Dalhousie University,
5850 College Street,
Halifax, NS B3H 1X5, Canada

A. G. Casson
Department of Surgery, University of Saskatchewan,
Royal University Hospital,
Saskatoon, SK S7N 0W8, Canada

Shuo Cheng Zhang received his Dr. rer. nat./PhD in molecular biology and plant virology from the University of Stuttgart, Stuttgart, Germany. He is presently an Assistant Professor of Biotechnology at the Center for Biotechnology and Genomics at Alcorn State University, Mississippi, USA. His research interests center on understanding virus–host cell interactions that underlie diseases of humans and plants.

Paul Murphy received his PhD in Physiology from Dalhousie University, Halifax, N.S., Canada. He is presently Professor and Head of the Department of Physiology and Biophysics at Dalhousie University. His research focuses on the role of endogenous antisense RNA in the regulation of gene expression.

nuclei. Although we found a trend towards reduced disease-free survival in patients with FGF-2 overexpressing esophageal adenocarcinomas, significantly worse disease-free survival was noted among patients whose tumors did not also overexpress the FGF-AS *b* isoform ($p$=0.03). Tetracycline-inducible FGF-AS *b* expression in stably transfected human Seg-1 esophageal adenocarcinoma cells resulted in a significant suppression of steady state FGF-2 mRNA content and cell proliferation. Our data implicate the FGF-AS *b* isoform in modulation of FGF-2 expression and clinical outcome in esophageal adenocarcinoma.

**Keywords** Fibroblast growth factor · FGF2 · Antisense gene expression · Esophageal adenocarcinoma · RNA splicing

## Introduction

The basic fibroblast growth factor (FGF-2) gene maps to human chromosome 4q26, a region of frequent gain or loss [1, 2] in human esophageal cancer. FGF-2 and FGF-AS/GFG are the "sense" and "antisense" products (respectively) of this bidirectionally transcribed gene locus (Fig. 1a). FGF-2, the prototypic member of a family of related genes encoding heparin-binding proteins with growth-, anti-apoptotic- and survival-promoting activity [3], has also been shown to contribute to malignant progression by increasing genetic instability [4] and resistance to anticancer drugs [5]. The FGF-AS RNA, which has been implicated in the regulation of FGF-2 expression and cell proliferation [6–9] is alternatively spliced, resulting in at least six alternatively spliced RNAs (designated *a–f*; Fig. 1). Four of these (*a–d*) contain open reading frames (ORFs) encoding isoforms of a novel nudix-motif protein called GFG. The nudix box motif is a signature sequence characteristic of a diverse family of enzymes that catabolize oxidized nucleotides and other potentially toxic compounds [10]. The two longest ORFs (GFG*a* and GFG*b*) predict proteins of 35 and 25 kDa, respectively. GFG*c* and -*d* differ only in their 3′ untranslated regions, and each predicts an N-terminally truncated GFG protein product of 18.2 kDa (Fig. 1b). All four transcripts are complementary to the FGF-2 transcript and may play a role in the antisense regulation of FGF-2.

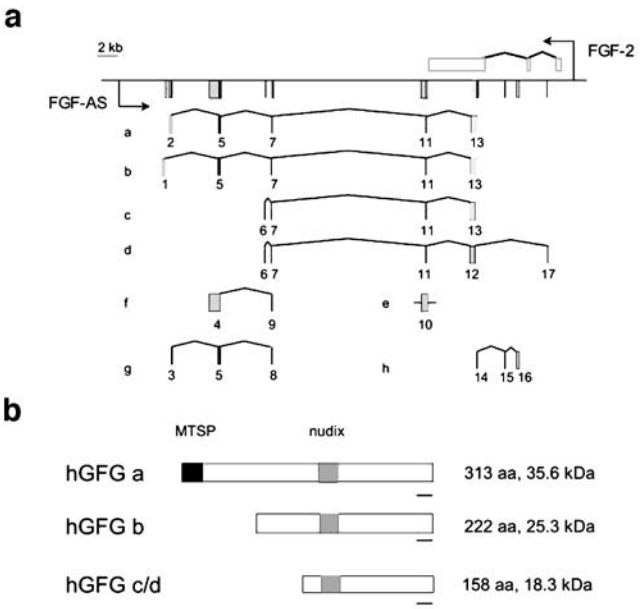


**Fig. 1** Organization of the human FGF-2/FGF-AS gene locus, alternative splicing of FGF-AS transcripts and predicted protein products. **a** Exons 11 and 13 of the FGF-AS gene are complementary to the 3′ UTR of FGF-2. FGF-AS splice variants *c* and *d* have a common open reading frame and differ only in their untranslated tails. FGF-AS transcripts *f–h* identified in dbEST do not contain open reading frames and appear to be incomplete. **b** The predicted translation products encoded by FGF-AS transcripts *a*, *b* and *c*/*d*, are aligned against the common nudix motif (*hatched box*). The *black box* indicates the potential mitochondrial targeting sequence (MTS). The *black line* indicates the region recognized by the anti-GFG antibody

We have recently demonstrated that overexpression of FGF-2 is associated with a significantly increased risk for tumor recurrence and reduced survival after surgical resection of esophageal cancer [11]. These risks are ameliorated in tumors co-expressing the endogenous FGF antisense RNA (FGF-AS/GFG), supporting our hypothesis that GFG is a novel tumor suppressor modulating the effects of FGF expression. These observations suggest that FGF-2/GFG expression is an important prognostic indicator for esophageal cancer and identify FGF-2 as a potential therapeutic target in the treatment of this disease. However, the significance of the FGF-AS RNA alternative splice variants and their encoded proteins in regulation of FGF-2 expression in human malignancy is unknown. With the goal of ultimately determining the biological function of FGF-AS/GFG, we focused here on elucidating the expression and subcellular distribution of the various FGF-AS/GFG isoforms in various human tissues, cell lines, and solid tumors, including primary esophageal adenocarcinoma (EADC), a tumor of increasing incidence and poor prognosis.

## Materials and methods

### Plasmid construction

Standard molecular cloning techniques were used as described elsewhere [12]. For construction of human GFG: GFP fusions and deletion mutants for expression in mammalian cells, the cDNA fragments of the coding regions were amplified with polymerase chain reaction (PCR) using Pfu DNA polymerase (Stratagene, La Jolla, CA) and template plasmid DNA pOTB7-NUDT6 [13] [American

Type Culture Collection (ATCC), Manassas, VA] with sequence-specific primers containing *Kpn*I and *BamH*I restriction sites. The resulting PCR products were ligated into the corresponding sites of mammalian expression vector pEGFP-N1 (Clontech, Mountain View, CA, USA). For bacterial MutT complementation assays, the cDNAs coding for GFG isoforms were PCR-amplified and ligated into vector pTrc99A [14] (kindly provided by Drs. W. Xu and M. J. Bessman, Department of Biology and the McCollum-Pratt Institute, The Johns Hopkins University, USA). A deletion mutant of human GFG lacking the Nudix domain was generated by two-step PCR and employed as described before [15]. pTrc99AmutT, containing a bacterial expression cassette of *Escherichia coli* MutT protein was isolated from the bacterial strain SB3 (generous gift of Dr. Bessman).

All constructs were amplified in *E. coli* DH5α (Invitrogen) and verified by restriction digestion. Positive clones were sequenced from both 5′- and 3′- directions to ensure ORF integrity with a Beckman CEQ8000 capillary sequencer (Beckman Coulter, Fullerton, CA). Plasmid DNAs were isolated with QIAfilter Plasmid Maxi/Midi Kit (Qiagen) for transfection/transformation.

## MutT complementation assay

GFG expression constructs were transformed into *E. coli* strain SB3 lacking a functional *mutT* gene [16], a generous gift from Dr. M. J. Bessman, Department of Biology and the McCollum-Pratt Institute, The Johns Hopkins University, USA. The complementation assays were conducted as described [17]. Briefly, the phenotype of SB3 strain was confirmed by its high frequency of mutation to antibiotic resistance in the presence of nalidixic acid. Single colonies of transformants were cultured overnight in 2.5 ml Luria–Bertani (LB) containing 100 μg/ml ampicillin and 1 mM isopropyl *b*-D-1-thiogalactopyranoside (IPTG). The overnight cultures were diluted to $10^{-6}$, from which 100 μl was streaked on the LB plates containing 25 μg/ml nalidixic acid and incubated at 37°C overnight. Each transformant chosen was streaked on three plates. Transformants transfected with pTrc99A, and pTrc99AMutT were used as the negative and positive controls, respectively. The number of colonies resistant to nalidixic acid were compared among the transformants transfected.

## Culture, transfection, and treatment of mammalian cells

C6, COS-7, and 293T cells (ATCC) were maintained in Dulbecco's modified Eagle's medium (DMEM) (Invitrogen) supplemented with 100 μg/ml streptomycin and penicillin, and 10% fetal calf serum (Invitrogen) at 37°C in a humidified atmosphere with 5% $CO_2$. The human esophageal adenocarcinoma cell line Seg-1 (a generous gift from David Beer PhD, University of Michigan, Ann Arbor MI, USA) was cultured as previously described [11]. Stable transfections were performed using Lipofectamine™ reagent (Invitrogen) according to the manufacturer's instructions, and transformants were selected in medium containing 1 mg/ml G418 (Invitrogen). Transient transfections were conducted using transfection reagents FuGENE 6 (Roche Applied Science) or GeneJuice™ (Novagen).

## Protein extraction, subcellular fractionation, and Western blotting

Total cell lysates and mitochondrial vs non-mitochondrial (cytoplasm + nuclei) fractions were isolated in the presence of protease inhibitors (Halt™ Protease Inhibitor Cocktail) using the Mitochondrial Isolation Kit (Pierce Biotechnology, Rockford, IL). For Western blot detection of fusion proteins and their dimers, total cellular protein was extracted using the Mitochondria Isolation Kit (Pierce Biotechnology, Rockford, IL) according to the manufacturer's instructions for isolation of mitochondria, with some modifications. Briefly, after step 5, the cell lysates were passed gently eight times through 21 g needles and then centrifuged at 700×*g* for 10 min at 4°C. The supernatant was transferred to a new tube and boiled for 5 min resulting in the final protein extract. One-tenth of the buffers used for isolation of mitochondria from $2\times10^7$ cells were employed for isolation of the total proteins from cells of two wells of a six-well plate. The Halt™ Protease Inhibitor Cocktail (Pierce Biotechnology, Rockford, IL) was added into the buffer A and C at 1:100, immediately before use. Mitochondrial and non-mitochondrial (cytoplasm + nuclei) fractions were isolated using the Mitochondria Isolation Kit (Pierce Biotechnology, Rockford, IL) following the manufacturer's instruction.

Protein extracts and subcellular fractions were subjected to sodium dodecyl sulfate-polyacrylamide gel electrophoresis (SDS-PAGE) using a NuPAGE® Electrophoresis System and 4-12% NuPAGE® Novex Bis-Tris-Gels (Invitrogen) and transferred to nitrocellulose membrane (Pierce Biotechnology, Rockford, IL) for immunoblotting. Immunodetection of GFG: GFP fusion proteins was performed using a mouse monoclonal anti-GFP antibody (A.V. Monoclonal Antibody of BD Living Colors™ Antibodies, BD Biosciences). The HSP60 antibody was a goat affinity-purified and pre-absorbed polyclonal antibody raised against a peptide mapping at the amino terminus of human HSP 60 of human origin (Santa Cruz Biotechnology). The rabbit polyclonal anti-GFG antibody raised against a peptide of the C-terminal rat GFG was described previously [7]. The secondary antibodies were a blotting grade affinity purified goat anti-mouse IgG (H + L) horseradish peroxidase conjugate (*Bio-Rad laboratories*), a bovine anti-goat IgG conjugated with horseradish peroxidase

(Santa Cruz Biotechnology), and a donkey anti-rabbit IgG-Fab' conjugated with horseradish peroxidase (Amersham). Signals were visualized by ECL using a SuperSignal® West Dura extended duration substrate kit (Pierce Biotechnology, Rockford, IL).

### Fluorescence microscopy

Stably transfected C6 cells were seeded in a four-well collagen I-coated Lab-Tek® II Chambered Coverglass (Nalge Nunc) containing DMEM supplemented with 10% fetal bovine serum (FBS) and incubated overnight at 37°C in a humidified atmosphere with 5% $CO_2$. For mitochondrial staining, the medium was changed to DMEM containing 100 nM MitoFluor Red 589 (MitoTracker, Molecular Probes, Eugene, OR), incubated for 30 min, and then replaced with normal medium without MitoTracker. The subcellular localization of the GFG:GFP fusions in the live cells was monitored with a ZEISS LSM 510 META laser scanning confocal microscope (LSCM, Carl Zeiss AG, Germany). Fluorescent image stacks were taken from a cell and analyzed using the software supplied (3D for LSM, Carl Zeiss AG).

For analysis of the subcellular localization of the GFG:GFP fusion proteins transiently expressed in C6, 293T, and Cos-7, cells were seeded in chambered coverslips containing DMEM supplemented with 10% FBS and incubated overnight, then transfected with the plasmid DNAs using FuGENE 6 transfection reagent. Six hours after transfection, the medium was replaced with the normal growth medium DMEM and cultured overnight. Mitochondrion staining and LSCM analysis were similar to that described for mitochondrion staining of stably transfected cell.

### RNA expression analysis in human tissues

Primary human samples were from the BD Multiple Tissue cDNA panels (BD Biosciences, Mississauga, ON). Amplification was performed using EnzyPlus 2000 polymerase system (EnzyPol). Each reaction was comprised of 2.5 μl of 10× buffer, 0.5 μl 10 mM deoxyribonucleotide triphosphates (dNTPs), 1.1 μl 50 mM $MgCl_2$, 1 μl 10 pmol/μl each forward/reverse primers, 0.5 μl Taq polymerase, and 16.4 μl $ddH_20$ for a final volume of 25 μl. For each reaction, 2 μl cDNA was added to be amplified. All reactions were carried out in MJ Research PTC-100 thermal cycler. Cycle conditions followed an initial denaturation step of 94°C for 4 min and 29 (GAPDH) or 38 (GFG-A/B/C) cycles of denaturation at 94°C for 45 s, annealing at 59.5°C for 55 s, and elongation at 72°C for 55 s followed by a final elongation at 72°C for 5 min. Amplification products were resolved on 1.8% agarose gels and visualized with ethidium bromide staining. PCR primers for glyceraldehyde-3-phosphate dehydrogenase (GAPDH) were as follows: forward GAPDH primer 5′-GAGCTGAACGG GAAGCTCACTGGC-3′, reverse GAPDH primer 5′-CCATGAGGTCCACCACCCTGTTGC-3′, for GFG-A, the forward primer was 5′-AATTAAGCGGCGTGGA GAT-3′ and GFG-A reverse was 5′-AATACAGCTCCTG CAACTCCTACTT-3′, for GFG-B, the forward primer was 5′-GCTGTAACGGCATCTGTGAA-3′ and GFG-B reverse was 5′-AATACAGCTCCTGCAACTCCTACTT-3′, for GFG-C, the forward primer was 5′-GCTTCTAGAACT GAGCTGTATTTGA-3′ and GFG-C reverse was 5′-GCTGGAAGTTCTTCCACAGTC-3′.

All PCR products were obtained within the linear range of the reaction, as previously described [7].

### Immunohistochemical analysis of human tissues

A modified immunoperoxidase technique was used to study the cellular distribution of GFG protein in formalin-fixed, paraffin-embedded panels of various human solid tumors and matched histologically normal tissues (Imgenex Histoarray, BIO/CAN Scientific, Mississauga, ON) as previously described [18]. Controls, including known positive and negative staining tissues and samples in which the primary antibody was omitted, were run in parallel with the test sections. The polyclonal anti-GFG antibody has been described in detail elsewhere [7]. The antigen was a KLH-coupled peptide corresponding to the COOH-terminal amino acids of the rat GFG. This sequence is common to all three isoforms and conserved across vertebrate species. The antibody has been validated for use in Western blot and immunohistochemistry of human tissues [18]. Immunoreactivity was evaluated independently by two investigators, noting subcellular distribution (nuclear or cytoplasmic) of GFG. To overcome the issue of tissue heterogeneity and to minimize subjectivity, a validated scoring system comprising both the fraction of immunopositive cells and intensity of staining was assigned to each tissue section, as previously reported [18–20]. Each coded tissue section was scored by two investigators at a double-headed microscope, evaluating intensity of immunoreactivity and the proportion of immunopositive cells, and a composite score, comprising the sum of the intensity and proportion scores, was then assigned to each tissue section. Briefly, each tissue section was assigned a score based on intensity of staining (0, none; 1, weak; 2, intermediate; 3, strong) and proportion of immunopositive cells (0, none; 1, less than one-hundredth; 2, one-hundredth to one-tenth; 3, one-tenth to one-third; 4, one-third to two-thirds; 5, greater than two-thirds). Overall immunoreactivity was then expressed as the sum of the intensity and proportion scores (range, 0 and 2–8). Tissues were considered negative with a composite score of 0, 2, or 3 (thereby avoiding false-positive results from occasional immuno-

positive cells). Tissues were considered weakly positive with a composite score of 4 to 6 and strongly positive with a score of 7 or 8. The subcellular distribution of each protein (cytoplasmic, nuclear, or both) was recorded [18–20].

### GFG isoform expression in esophageal adenocarcinomas

We studied GFG isoform expression (RNA and protein) in a subset of patients with primary EADC, defined according to strict clinicopathologic criteria, for whom tissues (tumor and matched histologically normal esophageal epithelium, stored in liquid nitrogen at −80°C) were available from our esophageal tumor bank, each with correlative clinical, histopathologic, staging, and outcomes data [11]. Follow-up was complete for all patients until July 2006. Differences in the frequency of FGF-AS and GFG isoform expression, according to demographic and clinicopathologic factors (age, gender, tumor differentiation, stage), were tested with a Chi-square test, with a Fisher exact test used if a cell contained fewer than five patients. Levels of FGF-AS mRNA expression in tumors, relative to matched histologically normal esophageal epithelia, were stratified as previously reported [11]; specifically: underexpression (ratio<0.7), the same (ratio=0.71-1.5), or overexpression (ratio>1.5). The prognostic importance of FGF-AS mRNA and GFG isoform expression in tumors (underexpressed vs same vs overexpressed; underexpressed/same vs overexpressed; underexpressed vs same/overexpressed) for overall and disease-free survival was examined in a univariate analysis with Kaplan–Meier survival methods and tested with the log-rank test. Multivariate analysis using Cox proportional hazards was then used to adjust for the effects of age, gender, tumor grade, and stage. Statistical significance was set at $p=0.05$ and all analyses were performed using SPSS for Windows 13.0 (SPSS, Chicago, IL).

All participating patients gave full informed consent, and collection and storage of resected esophageal tissues was in accordance with the 1998 Canadian Tri-Council Policy "Statement on Ethical Conduct for Research Involving Humans". Approval to study banked esophageal tissues was approved by the Health Sciences and Humanities Research Ethics Board at Dalhousie University (2002-539).

## Results

### Computational analysis of *fgf-as* RNA products

The organization of the human *FGF-2*/*GFG* gene locus is depicted in Fig. 1a. The locus, which maps to chromosome 4q26 [9], is bidirectionally transcribed to produce one FGF-2 mRNA and multiple alternatively spliced FGF-antisense (FGF-AS) RNAs (Fig. 1a). At least eight complete or partial FGF-AS RNAs, designated "*a*" through "*h*" can be identified in GenBank and dbEST databases [21]. The four longest splice variants (*a*, *b*, *c*, and *d*) share significant regions of complementarity with the FGF-2 mRNA. These splice variants also contain open reading frames encoding three isoforms of a novel nudix-motif protein called GFG (Fig. 1b). Blast alignments of the human GFG proteins with NCBI databases identify a variety of closely related homologs in many species across the animal kingdom (Fig. 2a). The results show that GFG is highly conserved, especially among vertebrates, with over 50% identity and 80% similarity at the amino acid level. The sense–antisense organization of the FGF-2/GFG gene locus is also highly conserved among vertebrates, suggesting an important functional interaction.

TargetP (TargetP Server v1.01 [22, 23]) and iPSORT [24], LOCtree [25] analysis of the amino acid sequence of hGFGa identified a putative N-terminal signal peptide or subcellular compartment targeting presequence. Further analysis using MitoProt [26] suggests that the N-terminal signal peptide of the hGFGa isoform, but not the hGFGb or hGFGc isoforms, contains a putative mitochondrial targeting sequence or MTS and a potential mitochondrial processing peptidase cleavage site between residue 28 and 29 (Fig. 2a). The N-terminal region of hGFGa had a high content of positively charged residues (18% in the MTS vs 12% on average) and hydrophobic and hydroxylated amino acid residues. Secondary structure prediction with ANTHEPROT [27] indicates that residues 7–18 of the hGFGa N terminus has the potential to form a putative amphiphilic-helix (data not shown). These features are common to several well characterized mitochondrial translocation signals [28, 29]. Comparison of other GFG protein sequences from public databases identified 12 GFG homologues from various animal species including insects, which bear an N-terminal MTS, whereas GFG homologues from plants do not. Except for the MTS and the conserved nudix signature sequence, no other functional motifs or subcellular localization signal sequences were identified in any GFG homologues.

The nudix box motif is a consensus signature sequence ($GX_5EX_7REUXEEXGU$), where $X$ is any amino acid and $U$ represents one of the bulky hydrophobic amino acids, usually Ile, Leu, or Val [30, 31]. The major substrates of the nudix hydrolase enzymes are nucleoside diphosphates linked to some other moiety $X$, hence, the acronym "nudix" [30]. These enzymes are involved in "house-cleaning" or detoxification of potentially mutagenic nucleotide by-products of cell damage and apoptosis or other deleterious metabolic intermediates [30, 32]. The Human Genome Organization has approved the designation NUDT for this gene family, of which there are at least 26 in the human genome. The gene encoding human GFG is designated NUDT6.

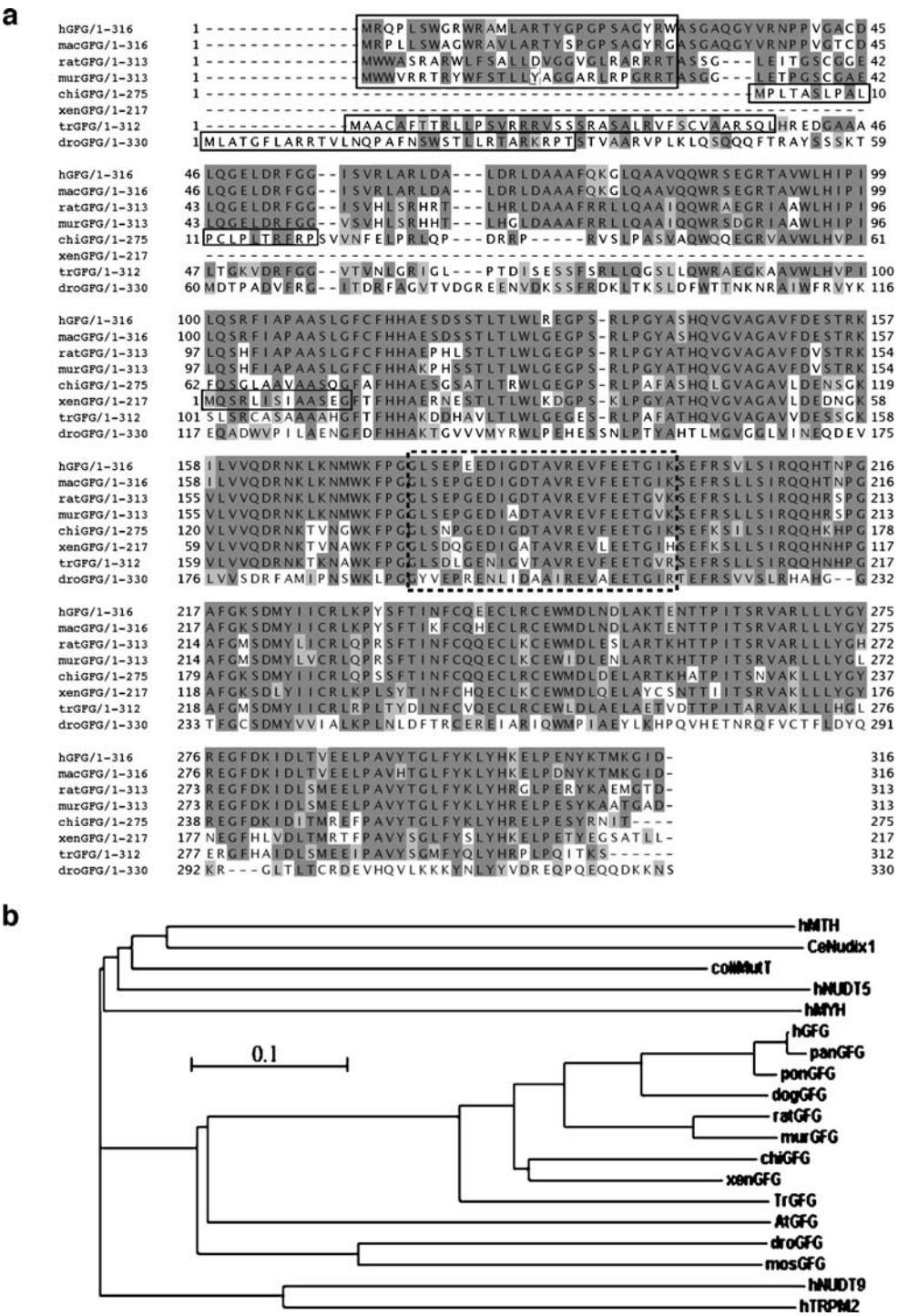


**Fig. 2** Alignment and phylogenetic analysis of GFG homologues. **a** Alignment of eight GFG homologues was performed with ClustalW (http://www.ebi.ac.uk/clustalw/). The predicted mitochondrial targeting signal peptides (MTSs) are outlined with *solid lines* and the conserved nudix domains are outlined with *dotted lines*. The putative cleavage sites of the mitochondrial signal peptidases are located after the last amino acid of the predicted MTSs. **b** The evolutionary relationships of 12 GFG protein sequences across species were compared with other prototypical Nudix proteins using ClustalW. The evolutionary distance is depicted with the total branch length (the bar = 0.1). *h Homo sapiens* (human), *mac Macaca mulata*, *rat Rattus norvegicus* (rat), *mur Mus musculus* (mouse), *chi Gallus gallus* (chicken), *xen Xenopus laevis*, *Tr Takifugu rubripes*, *dro Drosophila melanogaster* (fruitfly), *dog Canis familiaris*, *mos Anopheles gambiae* (malaria mosquito), *Ce Caenorhabditis elegans* (nematode), *At Arabidopsis thaliana*, *coli Escherichia coli*

The evolutionary relationships of GFG homologues with other nudix motif proteins are summarized in Fig. 2b. The prototypic *E. coli* antimutator protein MutT and its human homolog hMTH [33], which hydrolyze oxidized guanine nucleotides, form a distinct group which also includes the DNA glycosylase hMYH [34], the 8-oxo-dGDP hydrolase hNUDT5 [35] and the *Caenorhabditis elegans* Nudix-1. Similarly, the nudix ADP-ribose phosphohydrolases hNUDT9 [36] and hTRPM2 [37] are grouped together in a separate family. The data demonstrate that GFG homologues from a wide variety of plant and animal species are grouped into an evolutionarily distinct nudix hydrolase family. A more complex phylogenetic analysis of GFG homologues against all human nudix proteins (data not

shown) indicates that GFG homologs across species are more evolutionarily related to each other than to other nudix proteins from the same species.

## Subcellular distribution of human GFG isoforms

As discussed above, all vertebrate GFG homologues have an apparent N-terminal mitochondrial targeting sequence in their major transcript, which is absent in the alternatively spliced isoforms. Although human GFG cDNAs have been cloned [38, 39] and GFG expression in human tissue and cells has been reported [9, 18, 40, 41], the subcellular localization of the protein has not been described. To confirm the predicted N-terminal MTS experimentally, a hGFGa-GFP expression construct was generated and stably expressed in rat C6 glioma cells. The subcellular localization of hGFG-GFP was first analyzed by subcellular fractionation and Western blotting (Fig. 3a). Western blotting with a monoclonal anti-GFP antibody detected the predicted ~60 kDa hGFGa-GFP fusion protein in the cytoplasm and in isolated mitochondrial fractions (Fig. 3a, lane 4). In the cytoplasmic but not mitochondrial fractions, an apparent doublet of ~118 and 126 kDa was detected, consistent with the molecular mass of hGFGa homodimers without or with an intact MTS, respectively (Fig. 3a, lane 3). Dimerization of hGFG is consistent with the physiologically active form of many other nudix-motif proteins [42]. Free monomeric GFP (~ 27 kDa) was predominantly

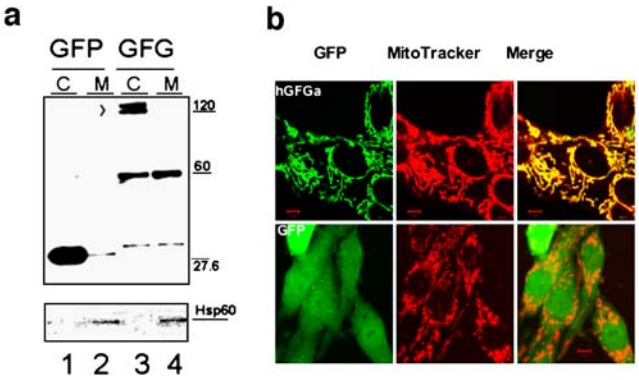


**Fig. 3** Expression and subcellular localization of human GFG isoform a. **a** A human GFGa-GFP fusion protein expression construct was stably transfected into rat C6 glioma cells and expression analyzed by Western blotting. Cell extracts were subjected to subcellular fractionation for isolation of mitochondrial (*M*) and non-mitochondrial fractions (*C*). After separation with SDS-PAGE (4–12% gradient polyacrylamide) proteins were immunodetected with a monoclonal anti-GFP antibody or a polyclonal antibody to heat shock protein Hsp60 as a molecular marker of the presence of mitochondria in the fractions. **b** C6 cells were stably transfected with plasmid DNAs expressing either free GFP or the human GFGa:GFP fusion and the subcellular localization of these products (*green*) and cellular mitochondria (*red*) were imaged separately as described in the Materials and methods section. The merged images (*yellow*) indicate colocalization of the GFG fusion proteins and the MitoTracker dye in mitochondria

detected in the cytoplasmic fraction (Fig. 3a, lane 1 vs 2), indicating that the mitochondrial targeting of GFP required the hGFGa fusion. The purity of the isolated mitochondrial fraction was confirmed by immunodetection of the mitochondrial molecular marker Hsp60 (Fig. 3a, lower panel).

The mitochondrial localization of the hGFGa-GFP fusion protein was further confirmed by imaging in conjunction with MitoTracker dye by dual monitoring of the red and green fluorescence in live cells using confocal laser scanning microscopy. As shown in Fig. 3b, hGFGa-GFP was detected exclusively in mitochondrial-like structures, which co-stained with MitoTracker dye. In contrast, free GFP was diffusely distributed in the nucleus and cytoplasm, and excluded from the mitochondria (Fig. 3b, panel GFP). Expression of hGFGa-GFP in transiently transfected cells gave the same result (not shown), indicating that mitochondrial targeting of hGFGa:GFP was hGFGa-specific and independent of the transfection methods.

The hGFGa immunoreactivity seen in the cytosolic fraction (Fig. 3a, lane 3) is almost certainly of mitochondrial origin. The Mitochondrial Isolation Kit used in this study yields highly purified mitochondria, but does not remove all mitochondria from the remaining cytosolic fraction. The confocal immunofluorescence data, showing localization of GFGa exclusively to mitochondria (Fig. 3b) confirms this interpretation. Dimeric forms of hGFG were detected only under the mild detergent conditions required for separation of the cytosolic and intact mitochondrial fractions. The more stringent conditions required to lyse the mitochondria for SDS-PAGE disrupts these dimers (data not shown). The anti-GFP antibody is highly specific under the conditions used here and does not detect any bands in lysates from untransfected cells. Using a bacterial expression system, we have also observed that hGFG-HisTag forms homodimers under non-denaturing conditions, which are disrupted by dithiothreitol (DTT) and boiling (data not shown).

To confirm the role of the unique N terminus of the hGFGa isoform in mitochondrial targeting, we next examined the subcellular distribution of deletion constructs of hGFGa and of intact hGFGb and hGFGc constructs (Fig. 4a). To confirm that the predicted products of these constructs were appropriately translated and to investigate the possibility of dimer formation, expression was first evaluated by immunoblotting of whole cell lysates isolated from transiently transfected Cos-7 cells under gentle detergent conditions, as described in the Materials and methods section (Fig. 4b). A single monomeric band of GFP (~27 kDa) was detected in the whole cell lysates of GFP transfectants (Fig. 4b, lane 1). GFP-immunoreactive bands of the expected sizes, corresponding to GFP fusion products of hGFGb (53 kDa), hGFGc (43 kDa), hGFGaΔN41 (~59 kDa), and hGFGaΔN41/c (~41 kDa) were detected in the transfected Cos-7 cell lysates,

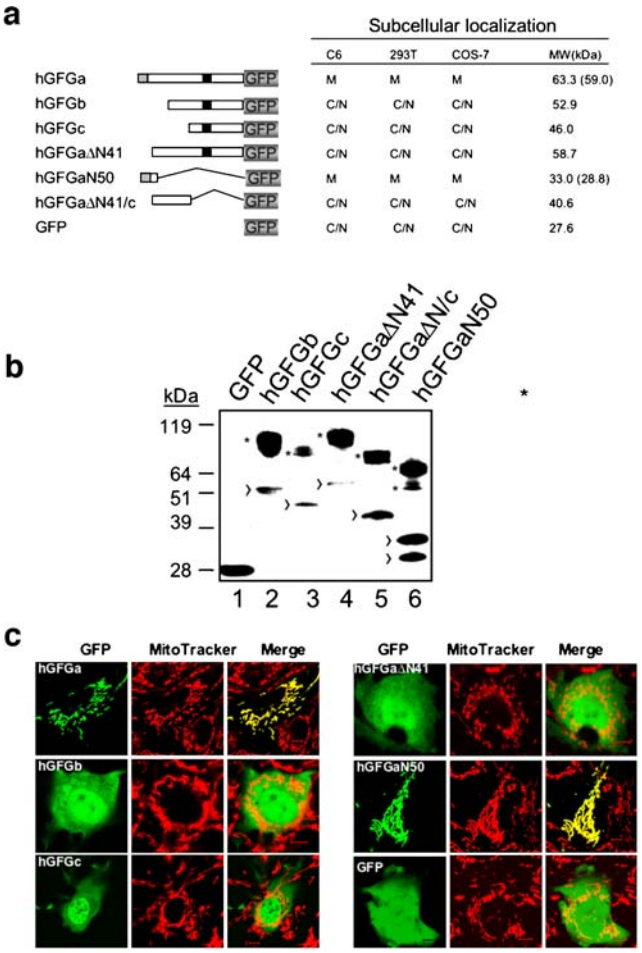


**Fig. 4** Expression and subcellular localization of human GFG isoforms and deletion mutants. **a** Schematic representation of human GFG-GFP fusion constructs. The *grey*, *black*, and *hatched boxes* represent the GFP, nudix, and mitochondrial targeting signal peptide domains, respectively. hGFGaΔ41is a deletion mutant of hGFGa, lacking the N terminal 41 amino acids. hGFGaN50 is a GFP construct containing only the N terminal 76 amino acids of hGFGa. hGFGaΔ41/c is a GFP construct of hGFGa in which the N terminal 41 aa and C terminal were removed. The subcellular localization of these GFG fusion products in C6 glioma cells, COS-7 cells, and 293T cells are summarized at the *right side of the panel*. The predicted molecular weights of the translation products are also indicated; the *numbers in brackets* indicate predicted molecular weight of products after cleavage of the N terminal MTS. **b** Immunodetection of GFP fusions of human GFG isoforms and their mutants transiently expressed in Cos-7 cells. Whole cell lysates subjected to SDS-PAGE (4–12% gradient polyacrylamide) followed by Western blotting with a monoclonal anti-GFP antibody. *Arrowheads* indicate the monomeric products of each construct. *Asterisks* indicate apparent dimeric forms

indicating that these proteins were expressed as designed (Fig. 4b, lanes 2–5). Interestingly, in the total protein extracts of cells expressing hGFGaN50 (expected size 33 kDa), two bands of ~29 and 33 kDa, were detected. The 33-kDa band corresponds to the expected size of hGFGaN50 containing the uncleaved MTS, whereas the ~29-kDa band is consistent with the predicted size of the cleaved form (Fig. 4b, lane 6). A common feature of proteins targeted to the mitochondrial matrix is that their N-terminal signal peptide is cleaved by a mitochondrial peptidase after import.

In addition to monomers of hGFGb, hGFGc, and hGFGaΔ41 (53, 46, and 59 kDa), larger bands corresponding to the predicted size of dimers (106, 92, and 118 kDa) were also detected (Fig. 4b, lanes: 2–4), indicating that the COOH-terminal amino acid sequence common to the three hGFG isoforms contains a potential dimerization domain. An apparent dimer of the hGFGaΔ41/c deletion mutant was also identified, suggesting that the N terminus of GFGa (which is unique to this isoform) is also involved in MTS-independent dimerization (Fig. 4b, lane 5). In the case of the hGFGaN50 construct, which contained only the MTS plus 22 additional N-terminal amino acids, two monomers were detected corresponding to the intact (33 kDa) and MTS-cleaved (29 kDa) forms. Apparent dimers of both products (~58 and 66 kDa) were detected, further supporting the suggestion that the N terminus of human GFG isoform a is also involved in dimerization and that this process does not require the MTS. Free GFP (28 kDa) was detected only in its monomeric form, confirming that the dimerization potential is an intrinsic property of GFG.

The construct lacking the predicted MTS (hGFGaΔN41; Fig. 4a) was excluded from mitochondria, indicating that the N-terminal 41 amino acids are necessary for mitochondrial localization of hGFGa (Fig. 4c, panel hGFGaΔN41). A GFG expression construct containing only the N-terminal 50 residues of hGFGa encompassing the predicted MTS (hGFGFaN50) targeted the GFP protein to mitochondria in C6 cells as efficiently as did full-length hGFGa (Fig. 4c, panels hGFGa vs hGFGFaN50). Similar results were obtained with both transient (Fig. 4c) and stable transfections (data not shown). Taken together, these results demonstrate that the predicted N-terminal MTS sequence of hGFGa is both necessary and sufficient for mitochondrial targeting hGFGa.

Human GFG isoforms b and c do not contain a predicted N-terminal MTS nor any other recognizable subcellular localization signals. Efforts to establish stable transfectants expressing GFP fusion constructs of hGFGb and hGFGc were unsuccessful, possibly reflecting antiproliferative actions of these isoforms. Consequently, only transient transfections were performed with these constructs. In C6 cells, both hGFGb and hGFGc were detected in the cytoplasm and nucleus, but not in mitochondria and nucleoli. The distribution of hGFGb and hGFGc in the cytoplasmic and nuclear compartments was variable, usually being intensely nuclear (Fig. 4c, panels hGFGb, hGFGc). However, in ~15% of transfected cells, hGFGb and hGFGc fusion products were more abundant in the

cytoplasm than in the nucleus (data not shown). Similar results were observed after transfection of COS-7 cells or human 293T cells (data not shown). Taken together, these data confirm that the mitochondrial targeting of GFG is isoform-specific and independent of cell lineage.

hGFG does not have MutT-like anti-mutator activity

The prototypic *E. coli* nudix protein MutT, and its human homologues, hydrolyze 8-hydroxy-dGTP (8-OH-dGTP) in vitro, and mutT gene deficiencies cause increased spontaneous A:T->C:G mutations [16, 43, 44]. Our phylogenetic and alignment analysis suggests that GFG is not evolutionarily related to orthologs of MutT hydrolases. However, we previously reported that rat GFG partially complemented MutT-deficient $SB^{MutT-}$ *E. coli*, suggesting a potential antimutator activity [45]. To determine whether the human GFG isoforms can complement MutT function, we cloned the open reading frames of human GFG isoforms a, b, c [13] and rat GFG [45] into the vector pTrc99A for conditional expression in an *E. coli* MutT1 deficient strain SB3 obtained from Dr. Maurice Bessman [46] and the complementation assay was conducted exactly as described [17]. Expression of wild-type MutT from plasmid pTrc99A-$MutT^{+}$ suppressed the mutator phenotype of the SB3 strain almost completely, whereas expression of human isoforms hGFGa, hGFGb, hGFGc, hGFGaΔNudix had no significant effect on the mutation frequency of SB3 strain (Table 1).

## Expression of GFG isoforms in human tissues

To determine if the predicted alternative splice variants of FGF-AS/GFG are indeed expressed in human tissues, PCR was performed using isoform-specific primer pairs to selectively amplify each of the major FGF-AS splice variants from a commercially available multitissue cDNA panels. As shown in Fig. 5a and b, GFG mRNA transcripts were detected in all tissues examined, although tissue-specific differences in isoform expression were observed. GFG*a* was expressed in a restricted subset of the tissues, most abundantly in pancreas and placenta. It was not

**Table 1** GFG does not complement MutT activity

| Plasmids | Nalidixic acid resistant colonies | | | |
|---|---|---|---|---|
| | Assay 1 | Assay 2 | Assay 3 | Mean |
| phGFGa | 403 | 529 | 820 | 584 |
| phGFGb | 805 | 627 | 387 | 606 |
| phGFGc | 740 | 1,101 | 1,420 | 1,087 |
| phGFGaΔNudix | 860 | 720 | 577 | 719 |
| prGFG | 690 | 682 | 257 | 543 |
| pTrc99AMutT$^{+}$ | 1 | 90 | 6 | 32 |
| pTrc99A | 250 | 668 | 560 | 493 |

SB3 (mutT1) cells transformed with pTrc99A alone as negative control, with pTrc99AMutT$^{+}$ as positive control, or with plasmids containing human GFG isoforms or its mutant or rat GFG were plated on nutrient agar with or without 25 μg/ml nalidixic acid. The numbers of the nalidixic acid resistant colonies in the table were the average of three plates for each assay. The average of the three assays is presented in the last column.

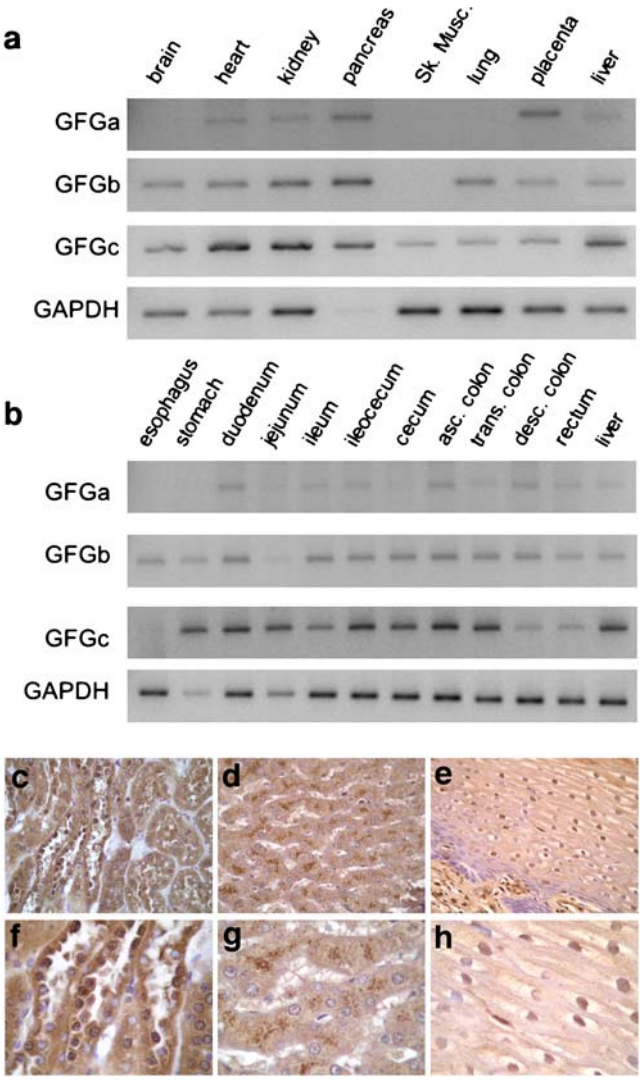


**Fig. 5** Tissue-specific expression of GFG in human tissues. **a**, **b** Expression of alternatively spliced GFG mRNA isoforms was detected with semiquantitative PCR. Expression level of GAPDH was used as reference. **c**–**h** Representative immunohistochemistry using a polyclonal antibody against a C terminal peptide, illustrating GFG protein expression in normal human kidney (**c**, low-power ×400; **f**, high power ×600), liver (**d**, low-power ×400; **g**, high power ×600), and esophagus (**e**, low-power ×400; **h**, high power ×600). Strong cytoplasmic and nuclear positivity was seen in the proximal and distal tubules of the kidney; cytoplasmic positivity only was seen in liver hepatocytes. In normal esophageal squamous epithelium, strong nuclear positivity (with weak cytoplasmic positivity) was seen in cells of the middle third layer, whereas no staining was seen in basal and parabasal cells

detectable in brain, skeletal muscle, lung, esophagus, or stomach. In contrast, hGFG*b* and hGFG*c* were more ubiquitously expressed.

Immunohistochemistry using a polyclonal antibody against the common C terminus of GFG/NUDT6 revealed that subcellular distribution of immunoreactivity was also tissue-specific (Fig. 5c–e; Table 2). GFG was primarily cytoplasmic in many tissues, including heart, pancreas, skeletal muscle, placenta, liver (Fig. 5, panels d,g), and large bowel. However, significant nuclear immunoreactivity was detected in brain, kidney, esophagus (Fig. 5, panels e,h), stomach, and small bowel. Both nuclear and cytoplasmic staining was observed in several tissues, including kidney (Fig. 5, panels c,f) and stomach. These observations suggest that GFG subcellular localization is tissue-specific and possibly isoform-dependent.

## FGF-AS RNA and GFG isoform expression in esophageal adenocarcinoma: associations with clinicopathological findings and survival

From our original series [11], tissue samples (all primary EADC and matched histologically normal esophageal epithelia) were available from only 24 patients (median age 62 years, range 51–79 years; 22 male, 2 female). At the time of last follow-up, six patients (25%) were alive and disease-free, with a median overall follow-up of 50 months.

**Table 2** Expression and subcellular distribution of GFG immunoreactivity in primary human tissues

| Tissue | Subcellular Localization | |
|---|---|---|
| | Cytoplasm | Nucleus |
| Brain | + | + |
| Heart | ++ | 0 |
| Kidney | +++ | + |
| Pancreas | + | 0 |
| Skeletal muscle | + | 0 |
| Placenta | + | 0 |
| Liver | +++ | 0 |
| Esophagus | + | +++ |
| Stomach | +++ | + |
| Small bowel | + | + |
| Large bowel | ++ | 0 |
| Rectum | 0 | + |

Immunohistochemistry was performed as described in the Materials and methods section. Briefly, immunoreactivity was evaluated independently by two investigators, noting subcellular distribution (nuclear or cytoplasmic) of GFG/NUDT6. To overcome the issue of tissue heterogeneity and to minimize subjectivity, a validated scoring system comprising both the fraction of immunopositive cells and intensity of staining was assigned to each tissue section, as previously reported [18–20]. Tissues were considered negative (0), weakly positive (+), moderately positive (++), or strongly positive (+++).

Median survival of patients who died with EADC was 15 months postoperative.

In normal esophageal squamous epithelia, weak nonspecific immunoreactivity for GFG protein was seen only in the cytoplasm of cells in the middle third layer, but not in cells of the basal or parabasal layers. In contrast, GFG protein was detected in the cytoplasm of all tumors and in 88% (21/24) of tumor cell nuclei. Relative to matched normal esophageal squamous epithelia, FGF-AS mRNA was underexpressed in 11 (46%) tumors, overexpressed in 8 (33%) tumors, and unchanged in 5 (21%) tumors. The dominant FGF-AS splice variant expressed in esophageal tissues was splice variant b. No associations were seen between expression of any FGF-AS transcript and GFG expression, age, gender, tumor differentiation (well, $n$=5; moderate, $n$=7; poor, $n$=12) or stage (IIA, $n$=7; III, $n$=16; IV, $n$=1). To increase the statistical power of the study, all subsequent survival analyses compared tumors overexpressing FGF-AS mRNA ($n$=8) vs those with the same/underexpression of FGF-AS mRNA ($n$=16).

As we had previously demonstrated FGF-2 overexpression to be a significant predictor of outcome after surgical resection of esophageal cancer, we first evaluated the effect of FGF-2 expression on survival in this subset of 24 patients with EADC. In keeping with our earlier observations, patients with tumors overexpressing FGF-2 mRNA had reduced overall and disease-free survival compared to those with tumors underexpressing FGF-2 (median 4 vs 27 months, respectively) (Fig. 6a). Although in this subset of patients, this effect did not reach statistical significance ($p$=0.12), this most likely reflects the smaller patient numbers in the current study. Similar to our previous findings, the overall level of expression of FGF-AS mRNA alone had no effect on survival, and furthermore, no association was seen between levels of expression of any individual FGF-AS isoform and survival. However, when the effect of expression of FGF-2 and each FGF-AS isoform in tumors was considered simultaneously, a significantly worse disease-free survival was noted among patients with tumors overexpressing FGF-2, which did not overexpress the FGF-AS *b* isoform ($p$=0.03) (Fig. 6b).

## Inducible expression of hGFG-b suppresses FGF-2 mRNA expression and inhibits growth of human Seg-1 esophageal adenocarcinoma cells

We have previously reported that the human Seg-1 esophageal adenocarcinoma cell line expresses FGF-2 mRNA [11]. To examine the effect of hFGF-AS/GFGb on FGF-2 mRNA expression, Seg-1 cells were stably transfected with a tetracycline-inducible construct directing the expression of hGFGb. After induction with doxycycline (DOX, 2 μg/ml) for 48 h, FGF-AS/GFG*b* and FGF-2 mRNA

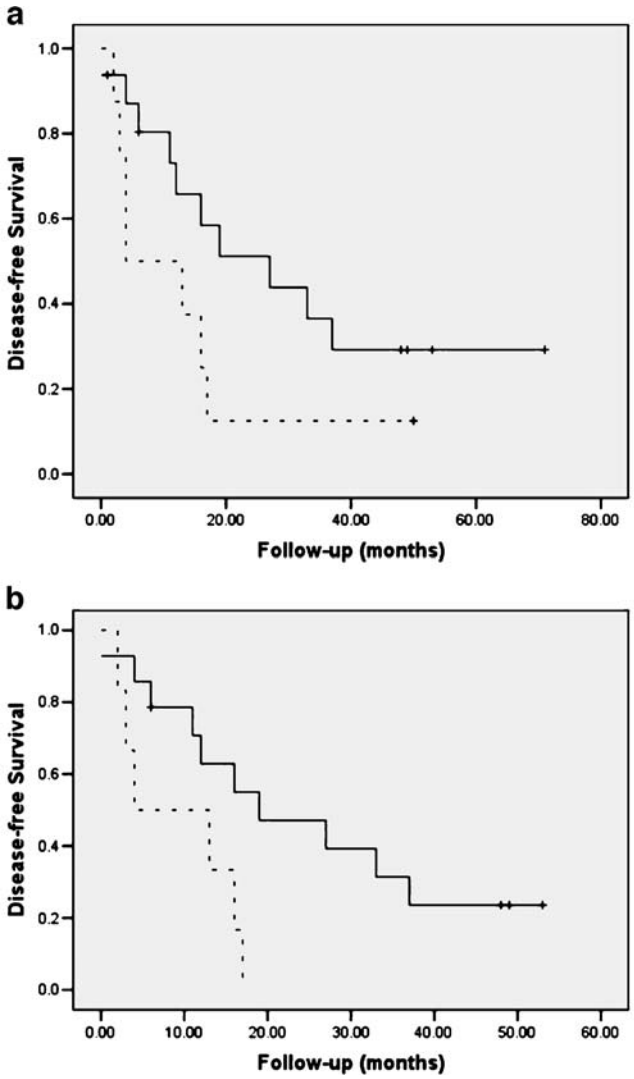


**Fig. 6** Kaplan–Meier disease-free survival curves for patients after surgical resection of esophageal adenocarcinoma, categorized by levels of expression of FGF-2 mRNA as determined by RT-PCR. In each figure, the *broken line* represents tumors with FGF-2 mRNA overexpression, and the *solid line* represents tumors with the same/underexpression of FGF-2 (relative to matched histologically normal esophageal epithelia). **a** Reduced disease-free survival was seen for patients (8/22) with tumors overexpressing FGF-2 mRNA (*broken line*), although this did not reach formal statistical significance ($p$= 0.12). **b** Disease-free survival curves illustrating the effect of expression of FGF-2 mRNA and the FGF-AS *b* isoform simultaneously. When the FGF-AS *b* was the same/underexpressed, a significantly worse disease-free survival was noted among patients with tumors overexpressing FGF-2 (*broken line*) compared to those with tumors with the same/underexpression of FGF-2 mRNA (*solid line*) ($p$=0.03)

expression were determined by reverse transcriptase (RT)-PCR. Doxycycline induction (2 μg/ml for 48 h) resulted in a nearly threefold induction of hGFG*b* mRNA abundance and a concomitant reduction in steady-state FGF-2 mRNA levels (Fig. 7a,b). Induction of FGF-AS/GFGb was also associated with a significant decrease in cell number over a 4-day culture period, and this was prevented by addition of exogenous FGF-2 to the culture medium (Fig. 7c).

## Discussion

The FGF antisense RNA has been implicated in the posttranscriptional regulation of FGF-2 expression and FGF-dependent tumor progression in esophageal adenocarcinoma. GFG/NUDT6 was originally identified as the antisense protein product of the FGF-2 gene [45], but its expression in human tissues has not been studied, and its function has remained elusive. While the growth-regulatory and tumor-suppressive effects of FGF-AS have been attributed to antisense RNA suppression of FGF-2 [8], there is also evidence to support the possibility of direct participation of the GFG protein, independent of FGF, in the control of cell proliferation [9]. It was therefore important to characterize the expression of FGF-AS splice variants, and their encoded GFG isoforms, in various normal human tissues including esophageal cancers.

Results presented here demonstrate that the primary FGF-AS mRNA is subject to a complex process of alternative splicing, resulting in multiple FGF-AS mRNA splice variants. Using a polyclonal antibody against the rat GFG C-terminal peptide, we have previously identified three immunoreactive bands of ~36, ~28, and ~18 kDa in human cell lines and tissues, consistent with the predicted translation products of these mRNAs [18]. FGF-AS mRNA expression is ubiquitous, although the individual splice variants were differentially expressed in a tissue-specific manner. The FGF-AS *a* variant was expressed in a limited set of tissues and was not detectable in brain, skeletal muscle, lung, esophagus, or stomach. The c variant was detected in all tissues examined, with the exception of esophagus, and was strongly expressed in heart, kidney, pancreas, and liver. The *b* variant was the predominant FGF-AS transcript expressed in normal esophagus and esophageal tumors. The subcellular distribution of GFG immunoreactivity was also tissue-specific and consistent with the tissue-dependent differential expression of these mRNA isoforms.

Our results demonstrate for the first time the structural basis for this isoform-specific subcellular distribution. Analysis of GFG sequences from many animal species identified a structurally conserved mitochondrial targeting sequence (MTS) in their N termini. We show here that the N terminus of human hGFGa contains a conserved MTS not present in hGFGb and hGFGc, and this MTS is both necessary and sufficient for mitochondrial localization. After mitochondrial import, the MTS is generally cleaved by mitochondrial processing peptidases [47]. The sizes of GFG:GFP fusion mutants observed in Figs 3 and 4 are consistent with MTS cleavage. These results also indicate

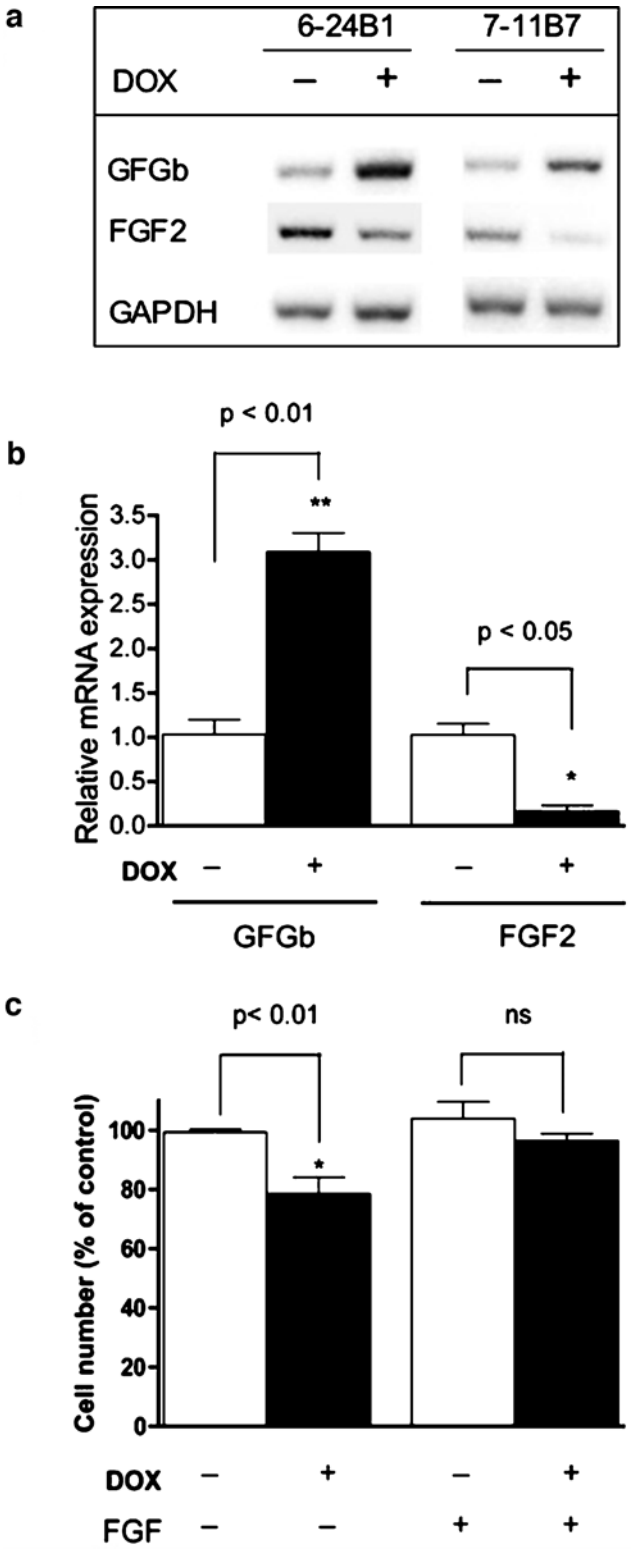


that the GFP fusion did not affect the structural conformation of the MTS [48].

In contrast, human hGFGb and hGFGc were localized in the nucleus and cytoplasm, consistent with the detection of GFG immunoreactivity in these compartments in various primary human tissues (Fig. 5 and [18]). In esophagus, which expresses only GFGb, immunoreactivity was almost exclusively nuclear (Fig. 5e,h), whereas in kidney, which expresses all three GFG mRNA species, immunoreactivity was detected in both the cytoplasmic and nuclear compartments (Fig. 5c,f). Previous immunohistochemical observations that GFG was localized in cytoplasm in some tissues and cell lines, while in nucleus in the others [9, 18, 45], are likely attributable to tissue-specific GFG isoform expression. Alternative splicing appears to be a common mechanism among human nudix motif proteins. The 24 Nudix motif genes identified in the human genome encode more than 100 alternatively spliced isoforms with varied subcellular distribution http://www.ncbi.nih.gov/IEB/Research/Acembly/ ).

The nudix box motif is a signature sequence characteristic of a large and diverse family of enzymes that catabolize potentially toxic compounds in the cell. The prototypic member of this family, the prokaryotic MutT protein, and its human homologue hMTH, are responsible for removing 8-oxo-dGTP from the nucleotide pool, thus, preventing transversion mutations arising from incorporation of oxidized guanine residues into DNA. Although phylogenetic analysis suggests that GFG is not an ortholog of bacterial MutT (Fig. 2), we had previously reported that rat GFG was able to partially complement MutT deficiency in the $SB^{MutT-}$ strain of *E. coli* [45]. In the present study, using a different bacterial strain (SB3), we were unable to detect any MutT-like activity in any of the three human nudix-containing GFG isoforms, nor with rat GFG (Table 1). These data suggest that under the conditions used here, GFG does not hydrolyze oxidized guanine nucleotides. Interestingly, NUDT3, which has no 8-oxo-dGTPase activity, was also able to partially complement MutT deficiency in the $SB^{MutT-}$ strain [49]. Clearly, mutation suppression in *E. coli*, by overexpression of mammalian enzymes, must be interpreted with caution. Recently, a GFG homolog from

◀ **Fig. 7** Effects of doxycycline-induced FGF-AS-*b* overexpression on FGF-2 mRNA expression and proliferation in Seg-1 esophageal adenocarcinoma cells. Seg-1 cells were stably transfected with the pTet-On plasmid and a construct containing the FGF-AS *b* cDNA fused to a Tet-responsive promoter. The steady-state level of FGF-AS *b* RNA and FGF-2 mRNA was determined by RT-PCR after 48 h culture in the absence (−) or presence (+) of doxycycline. **a** Representative RT-PCR results from two stably transfected Seg-1 lines. **b** Relative expression of FGF-AS b and FGF-2. **c** Effect of doxycycline and FGF on cell growth. Cells were incubated without (−) or with (+) doxycycline (2 μg/ml) in the absence or presence of recombinant FGF-2 (3 ng/ml). Cell numbers were determined after 4 days by MTT assay. The results are the mean ± SEM of four independent experiments

the plant *Aarabidopsis thaliana* (AtNUDT6; At2g04450), has been shown to have activity against ADP-ribose and NADH [50]. Free ADP-ribose is a potentially toxic metabolite generated from NAD via multiple metabolic pathways, most notably by degradation of poly(ADP-ribose) by nuclear and mitochondrial glycohydrolases. However, preliminary enzymatic analysis of hGFG failed to identify any typical nudix-like pyrophosphatase activity against a variety of substrates (A. G. McLennan, University of Liverpool, personal communication).

Although the precise function of the GFG protein remains unknown, our present results confirm and extend our earlier observation of a significant effect of FGF-AS RNA on FGF-2 overexpression and outcome after surgical resection of esophageal adenocarcinoma. The possibility that this is an antisense RNA-mediated effect is supported by the observation that a significantly worse disease-free survival was noted among patients with tumors overexpressing FGF-2, which did not overexpress the FGF-AS *b* isoform. Furthermore, our preliminary data indicated a reduction in steady-state FGF-2 mRNA levels after induced overexpression of FGF-AS *b* mRNA in esophageal adenocarcinoma cell lines, and this was associated with a small but significant deficit in cell growth. This is consistent with our recent demonstration that constitutive overexpression of the rat FGF-AS RNA suppressed FGF-2 expression [8] and significantly delayed S-phase progression in C6 glioma cells [51].

In summary, we have shown that GFG/NUDT6 is a highly conserved nudix motif protein present in all multicellular organisms. The demonstration that GFG/NUDT6 isoform a is, to a large extent, compartmentalized specifically to mitochondria in animal species (but not in plants), and the high level of conservation of the mitochondrial targeting sequence in animal GFG homologs suggests that this protein has evolved a unique role in the mitochondrial metabolism of multicellular animals. In addition, the FGF-AS/GFG mRNA appears to play a role in the antisense-RNA-mediated regulation of FGF-2 expression.

**Acknowledgements** We thank the Dalhousie Cancer Research and Training Program for postdoctoral fellowship support to SC Zhang. AG Casson and GA Porter were supported by a Clinical Research Scholarships from the Dalhousie University Faculty of Medicine. We also wish to thank Ms. R. Mi for excellent technical assistance and Dr. Mark Nachtigal for critical reading of the manuscript. This project was funded by grants from the Canadian Institutes of Health Research and the Cancer Research Society Inc.

## References

1. Rumpel CA, Powell SM, Moskaluk CA (1999) Mapping of genetic deletions on the long arm of chromosome 4 in human esophageal adenocarcinomas. Am J Pathol 154:1329–1334
2. Barnas C, Henn T, Stark M, Haas O, Romeo G, Montesano R, Hainaut P, Casson A (1999) Detection of genetic alterations in cancers of the esophagus and esophagogastric junction by comparative genomic hybridization: frequent involvement of chromosome 4q. Proceedings of the Am Assoc Cancer Res 1999, p 539
3. Powers CJ, McLesky SW, Wellstein A (2000) Fibroblast growth factors, their receptors and signaling. Endocr Relat Cancer 7:165–197
4. Huang A, Jin H, Wright JA (1994) Aberrant expression of basic fibroblast growth factor in nih-3t3 cells alters drug resistance and gene amplification potential. Exp Cell Res 213:336–339
5. Song S, Wientjes MG, Gan Y, Au JL-S (2000) Fibroblast growth factors: an epigenetic mechanism of broad spectrum resistance to anticancer drugs. Proc Natl Acad Sci (USA) 97:8658–8663
6. Murphy PR, Knee RS (1994) Identification and characterization of an antisense RNA transcript (gfg) from the basic fibroblast growth factor gene in human and rat cells. Mol Endocrinol 8:852–859
7. Knee R, Li AW, Murphy PR (1997) Characterization and tissue-specific expression of the rat basic fibroblast growth factor antisense mRNA and protein. Proc Natl Acad Sci USA 94:4943–4947
8. Li AW, Murphy PR (2000) Expression of alternatively spliced fgf-2 antisense RNA transcripts in the central nervous system: regulation of fgf-2 mRNA translation. Mol Cell Endocrinol 170:233–242
9. Asa SL, Ramyar L, Murphy PR, Li AW, Ezzat S (2001) The endogenous fibroblast growth factor-2 antisense gene product regulates pituitary cell growth and hormone production. Mol Endocrinol 15:589–599
10. Bessman MJ, Frick DN, O'Handley SF (1996) The mutt proteins or "nudix" hydrolases, a family of versatile, widely distributed, "housecleaning" enzymes. J Biol Chem 271:25059–25062
11. Barclay C, Li AW, Geldenhuys L, Baguma-Nibasheka M, Porter GA, Veugelers PJ, Murphy PR, Casson AG (2005) Basic fibroblast growth factor (fgf-2) overexpression is a risk factor for esophageal cancer recurrence and reduced survival, which is ameliorated by coexpression of the fgf-2 antisense gene. Clin Cancer Res 11:7683–7691
12. Sambrook J, Russell DW (2001) Molecular cloning: A laboratory manual. 3rd ed. Cold Spring Harbor Laboratory. Cold Spring Harbor, N.Y.
13. Strausberg RL, Feingold EA, Grouse LH, Derge JG, Klausner RD, Collins FS, Wagner L, Shenmen CM, Schuler GD, Altschul SF, Zeeberg B, Buetow KH, Schaefer CF, Bhat NK, Hopkins RF, Jordan H, Moore T, Max SI, Wang J, Hsieh F, Diatchenko L, Marusina K, Farmer AA, Rubin GM, Hong L, Stapleton M, Soares MB, Bonaldo MF, Casavant TL, Scheetz TE, Brownstein MJ, Usdin TB, Toshiyuki S, Carninci P, Prange C, Raha SS, Loquellano NA, Peters GJ, Abramson RD, Mullahy SJ, Bosak SA, McEwan PJ, McKernan KJ, Malek JA, Gunaratne PH, Richards S, Worley KC, Hale S, Garcia AM, Gay LJ, Hulyk SW, Villalon DK, Muzny DM, Sodergren EJ, Lu X, Gibbs RA, Fahey J, Helton E, Ketteman M, Madan A, Rodrigues S, Sanchez A, Whiting M, Young AC, Shevchenko Y, Bouffard GG, Blakesley RW, Touchman JW, Green ED, Dickson MC, Rodriguez AC, Grimwood J, Schmutz J, Myers RM, Butterfield YS, Krzywinski MI, Skalska U, Smailus DE, Schnerch A, Schein JE, Jones SJ, Marra MA (2002) Generation and initial analysis of more than 15,000 full-length human and mouse cDNA sequences. Proc Natl Acad Sci USA 99:16899–16903
14. Amann E, Brosius J, Ptashne M (1983) Vectors bearing a hybrid trp-lac promoter useful for regulated expression of cloned genes in *Escherichia coli*. Gene 25:167–178
15. Zhang SC, Wege C, Jeske H (2001) Movement proteins (bc1 and bv1) of abutilon mosaic geminivirus are cotransported in and between cells of sink but not of source leaves as detected by green fluorescent protein tagging. Virology 290:249–260
16. Bhatnagar SK, Bessman MJ (1988) Studies on the mutator gene, mutt of *Escherichia coli*. Molecular cloning of the gene,

purification of the gene product, and identification of a novel nucleoside triphosphatase. J Biol Chem 263:8953–8957
17. Xu W, Gauss P, Shen J, Dunn CA, Bessman MJ (2002) The gene e.1 (nude.1) of t4 bacteriophage designates a new member of the nudix hydrolase superfamily active on flavin adenine dinucleotide, adenosine 5′-triphospho-5′-adenosine, and adp-ribose. J Biol Chem 277:23181–23185
18. Baguma-Nibasheka M, Li AW, Osman MS, Geldenhuys L, Casson AG, Too CK, Murphy PR (2005) Coexpression and regulation of the fgf-2 and fgf antisense genes in leukemic cells. Leuk Res 29:423–433
19. Casson AG, Zheng Z, Evans SC, Geldenhuys L, van Zanten SV, Veugelers PJ, Porter GA, Guernsey DL (2005) Cyclin d1 polymorphism (g870a) and risk for esophageal adenocarcinoma. Cancer 104:730–739
20. Casson AG, Tammemagi M, Eskandarian S, Redston M, McLaughlin J, Ozcelik H (1998) P53 alterations in oesophageal cancer: association with clinicopathological features, risk factors, and survival. Mol Pathol 51:71–79
21. Thierry-Mieg D, Thierry-Mieg J, Potdevin M, Sienkiewicz M (2004) Identification and functional annotation of cDNA-supported genes in higher organisms using Aceview. (hum nov 04 release). In: http://wwwacevieworg/
22. Emanuelsson O, Nielsen H, Brunak S, von Heijne G (2000) Predicting subcellular localization of proteins based on their n-terminal amino acid sequence. J Mol Biol 300:1005–1016
23. Nielsen H, Engelbrecht J, Brunak S, von Heijne G (1997) Identification of prokaryotic and eukaryotic signal peptides and prediction of their cleavage sites. Protein Eng 10:1–6
24. Bannai H, Tamada Y, Maruyama O, Nakai K, Miyano S (2002) Extensive feature detection of n-terminal protein sorting signals. Bioinformatics 18:298–305
25. Nair R, Rost B (2005) Mimicking cellular sorting improves prediction of subcellular localization. J Mol Biol 348:85–100
26. Claros MG, Vincens P (1996) Computational method to predict mitochondrially imported proteins and their targeting sequences. Eur J Biochem 241:779–786
27. Deleage G, Combet C, Blanchet C, Geourjon C (2001) Antheprot: an integrated protein sequence analysis software with client/server capabilities. Comput Biol Med 31:259–267
28. von Heijne G (1985) Signal sequences. The limits of variation. J Mol Biol 184:99–105
29. von Heijne G (1986) Mitochondrial targeting sequences may form amphiphilic helices. Embo J 5:1335–1342
30. Bessman MJ, Frick DN, O'Handley SF (1996) The mutt proteins or "nudix" hydrolases, a family of versatile, widely distributed, "housecleaning" enzymes. J Biol Chem 271:25059–25062
31. Mildvan AS, Xia Z, Azurmendi HF, Saraswat V, Legler PM, Massiah MA, Gabelli SB, Bianchet MA, Kang LW, Amzel LM (2005) Structures and mechanisms of nudix hydrolases. Arch Biochem Biophys 433:129–143
32. McLennan AG (1999) The mutt motif family of nucleotide phosphohydrolases in man and human pathogens (review). Int J Mol Med 4:79–89
33. Cai J-P, Kawate H, Ihara K, Yakushiji H, Nakabeppu Y, Tsuzuki T, Sekiguchi M (1997) Significance of the conserved amino acid sequence for human mth1 protein with antimutator activity. Nucleic Acids Res 25:1170–1176
34. Kim CJ, Cho YG, Park CH, Kim SY, Nam SW, Lee SH, Yoo NJ, Lee JY, Park WS (2004) Genetic alterations of the myh gene in gastric cancer. Oncogene 23:6820–6822
35. Ishibashi T, Hayakawa H, Sekiguchi M (2003) A novel mechanism for preventing mutations caused by oxidation of guanine nucleotides. EMBO Rep 4:479–483
36. Lin S, Gasmi L, Xie Y, Ying K, Gu S, Wang Z, Jin H, Chao Y, Wu C, Zhou Z, Tang R, Mao Y, McLennan AG (2002) Cloning, expression and characterisation of a human nudix hydrolase specific for adenosine 5′-diphosphoribose (adp-ribose). Biochim Biophys Acta 1594:127–135
37. Perraud AL, Fleig A, Dunn CA, Bagley LA, Launay P, Schmitz C, Stokes AJ, Zhu Q, Bessman MJ, Penner R, Kinet JP, Scharenberg AM (2001) Adp-ribose gating of the calcium-permeable ltrpc2 channel revealed by nudix motif homology. Nature 411:595–599
38. Gagnon ML, Moy GK, Klagsbrun M (1999) Characterization of the promoter for the human antisense fibroblast growth factor-2 gene; regulation by ets in Jurkat T cells. J Cell Biochem 72:492–506
39. Murphy PR, Knee RS (1994) Identification and characterization of an antisense RNA transcript (gfg) from the human basic fibroblast growth factor gene. Mol Endocrinol 8:852–859
40. Knee RS, Pitcher SE, Murphy PR (1994) Basic fibroblast growth factor sense (fgf) and antisense (gfg) RNA transcripts are expressed in unfertilized human oocytes and in differentiated adult tissues. Biochem Biophys Res Commun 205:577–583
41. Mihalich A, Reina M, Mangioni S, Ponti E, Alberti L, Vigano P, Vignali M, Di Blasio AM (2003) Different basic fibroblast growth factor and fibroblast growth factor-antisense expression in eutopic endometrial stromal cells derived from women with and without endometriosis. J Clin Endocrinol Metab 88:2853–2859
42. Gabelli SB, Bianchet MA, Bessman MJ, Amzel LM (2001) The structure of adp-ribose pyrophosphatase reveals the structural basis for the versatility of the nudix family. Nat Struct Biol 8:467–472
43. Taddei F, Hayakawa H, Bouton M-F, Cirinesi A-M, Matic I, Sekiguchi M, Radman M (1997) Counteraction by mutt protein of transcriptional errors caused by oxidative damage. Science 278:128–130
44. Nakabeppu Y (2001) Molecular genetics and structural biology of human mutt homolog, mth1. Mutat Res 477:59–70
45. Li AW, Too CK, Knee R, Wilkinson M, Murphy PR (1997) Fgf-2 antisense RNA encodes a nuclear protein with mutt-like antimutator activity. Mol Cell Endocrinol 133:177–182
46. Xu W, Shen J, Dunn CA, Bessman MJ (2003) A new subfamily of the nudix hydrolase superfamily active on 5-methyl-utp (ribo-ttp) and utp. J Biol Chem 278:37492–37496
47. Pfanner N, Geissler A (2001) Versatility of the mitochondrial protein import machinery. Nat Rev Mol Cell Biol 2:339–349
48. Miura S, Amaya Y, Mori M (1986) A metalloprotease involved in the processing of mitochondrial precursor proteins. Biochem Biophys Res Commun 134:1151–1159
49. Chu C, Alapat D, Wen X, Timo K, Burstein D, Lisanti M, Shears S, Kohtz DS (2004) Ectopic expression of murine diphosphoinositol polyphosphate phosphohydrolase 1 attenuates signaling through the erk1/2 pathway. Cell Signal 16:1045–1059
50. Ogawa T, Ueda Y, Yoshimura K, Shigeoka S (2005) Comprehensive analysis of cytosolic nudix hydrolases in *Arabidopsis thaliana*. J Biol Chem 280:25277–25283
51. Baguma-Nibasheka M, Li A, Murphy PR (2007) The fibroblast growth factor-2 antisense gene inhibits nuclear accumulation of fgf-2 and delays cell cycle progression in c6 glioma cells. Mol Cell Endocrinol 267:127–136